Front. Optoelectron. 2016, 9(4): 599–608
DOI 10.1007/s12200-016-0549-8

RESEARCH ARTICLE

Design of four mirror inverted telephoto zoom system

Jun CHANG (✉)[1], Guijuan XIE[1], Lifei ZHANG[1], Yao XU[1], Jide ZHOU[1], Shengyi YANG[2]

1 School of Optoelectronic, Beijing Institute of Technology, Beijing 100081, China
2 School of Physics, Beijing Institute of Technology, Beijing 100081, China

Abstract A novel inverted telephoto four mirror zoom system with large field of view (FOV) was designed over a wide spectral bandwidth. The initial configuration of the zoom system was obtained by applying the aberration equations under certain constraints. Then, a method was presented to correlate the aspheric coefficients with the aberrations of this system. By using this method, the required image quality could be achieved after optimization using the ZEMAX® Optical Design Code. Besides good image quality, another benefits of using this system is the potential for using cheap optics.

Keywords geometric optical design, aberration compensation, lens system design, reflective zoom

1 Introduction

Mirror systems have many advantages, such as light weight, free of chromatic aberrations, high thermal stability, etc. Such optical systems have received considerable attention as a critical technique in aerospace systems. The way to design reflective zoom system has been developed since 1980s. During this period, the mirror optical zoom systems employed the mechanical devices to move one or more elements to vary the focal lengths, they did not have stable image surfaces, and the initial configuration designed more by experience. In 2009, Seidl et al. designed a mirror system without obscuration by changing the surface shape of the deformable mirror [1,2], then this kind of zoom systems that use active optical elements has developed, the active optical elements include spatial light modulators, liquid lens, and deformable mirror [3–7], but the variable scope are limited, and the price are expensive, they are mainly used in laboratory research at the present stage, mechanical zoom optical system has great prospect in practical application.

Received September 11, 2015; accepted December 23, 2015

E-mail: bitchang@bit.edu.cn

In these systems the problem of selecting their initial configurations remain unresolved. In 2008, Mikš et al. used the Seidel aberration equations to construct the initial configuration of a transmission-mode optical zoom system for the first time [8]. In 2010, Zhang et al. introduced another way to solve this problem based on the theory of Seidel aberrations, but it was not cost effective [9].

In this paper, we developed the analytical theory by using the Seidel aberrations under specific constraints and applied the ray tracing method to obtain the initial configuration for our proposed optical model. We finally obtained a diffraction limited image by developing a linkage between the aspheric coefficients and the aberrations and optimizing the optical system.

2 Design of the initial configuration of four-mirror system

For the sake of checking the correction of the theory, we made an experimental prototype. System parameters of the optical system are shown in Table 1. The primary aberration theory was applied to find the initial configuration of the mirror system. First, through ray tracing, an expression for the primary aberrations was obtained at different focal lengths of two configurations. Then, the initial configuration was evolved from the differential zoom theories and the primary aberration theory [9]. The four-mirror optical zoom system was optimized by

Table 1 System parameters of the optical system

system parameters	value
zoom ratio	3×
range of focal length	20–60 mm
zooming group	primary mirror
compensating group	fourth mirror
F/#	5
field of view (FOV)	7.2°–2.4°

combining the aspheric coefficients with the primary aberrations.

In Fig. 1, the second mirror (M2) is set as an aperture. The marginal and chief rays of this proposed optical zoom system are shown in Figs. 1(a) and 1(b) respectively. The marginal and chief rays are chosen to deduce the expression for primary aberrations, which is described as below [9–11]:

$$S_{ki} = S_{ki}(f_1, f_2, f_3, f_4, \beta_{2i}, \beta_{3i}, \beta_{4i}), \tag{1}$$

where i (= 1, 2) is the multiple configurations of the optical zoom system, k (= 1, 2, 3, 4) is the spherical, coma, astigmatism and the field curvature aberrations respectively, $\beta_{2i}, \beta_{3i}, \beta_{4i}$ are the magnification of M2,M3 and M4 of ith configuration, and f_1, f_2, f_3, f_4 are the focal length of the M1,M2,M3 and M4 respectively.

It is difficult to find the exact solution for the suitable initial configuration of the optical zoom system through Eq. (1). So it becomes mandatory to apply specific constraints.

We chose an inverted wide FOV telephoto configuration as a sample optical system. According to the matrix optics, the transfer matrix of the four mirror zoom system is as follows:

$$\begin{aligned}\boldsymbol{T} &= \boldsymbol{R}_4\boldsymbol{D}_3\boldsymbol{R}_3\boldsymbol{D}_2\boldsymbol{R}_2\boldsymbol{D}_1\boldsymbol{R}_1 \\ &= \begin{bmatrix} 1 & \varphi_4 \\ 0 & 1 \end{bmatrix} \begin{bmatrix} 1 & 0 \\ -d_{34}/n_3' & 1 \end{bmatrix} \begin{bmatrix} 1 & \varphi_3 \\ 0 & 1 \end{bmatrix} \begin{bmatrix} 1 & 0 \\ -d_{23}/n_2' & 1 \end{bmatrix} \\ &\quad \begin{bmatrix} 1 & \varphi_2 \\ 0 & 1 \end{bmatrix} \begin{bmatrix} 1 & 0 \\ -d_{12}/n_1' & 1 \end{bmatrix} \begin{bmatrix} 1 & \varphi_1 \\ 0 & 1 \end{bmatrix} \\ &= \begin{bmatrix} B & A \\ C & D \end{bmatrix},\end{aligned} \tag{2}$$

$$\varphi_k = \frac{n' - n}{r_k}, \tag{3}$$

$$d_{k,k+1} = (1-\beta_k)\frac{r_k}{2} + \left(\frac{1}{\beta_{k+1}} - 1\right)\frac{r_{k+1}}{2}. \tag{4}$$

The transfer matrix for the second, third and fourth mirrors is as follows:

$$\begin{aligned}\boldsymbol{T} &= \boldsymbol{R}_4\boldsymbol{D}_3\boldsymbol{R}_3\boldsymbol{D}_2\boldsymbol{R}_2 \\ &= \begin{bmatrix} 1 & \varphi_4 \\ 0 & 1 \end{bmatrix} \begin{bmatrix} 1 & 0 \\ -d_{34}/n_3' & 1 \end{bmatrix} \begin{bmatrix} 1 & \varphi_3 \\ 0 & 1 \end{bmatrix} \\ &\quad \begin{bmatrix} 1 & 0 \\ -d_{23}/n_2' & 1 \end{bmatrix} \begin{bmatrix} 1 & \varphi_2 \\ 0 & 1 \end{bmatrix} \\ &= \begin{bmatrix} B_{2-4} & A_{2-4} \\ C_{2-4} & D_{2-4} \end{bmatrix},\end{aligned} \tag{5}$$

where φ_k (k = 1,2,3,4) is the power of the mirror k; d_{ij} is the spacing between mirror i and mirror j; r_k is the radius of curvature of mirror k; n, n' are the refractive indices of the object and image space respectively; $A_{(2-4)i}$ (i = 1, 2) is the power of the second, third and the fourth mirror of configuration i.

The specific conditions are as follows:

$$\varphi_1 < 0,\ A_{(2-4)1} > 0,\ A_{(2-4)2} > 0. \tag{6}$$

After applying the constraint equation to the primary aberrations, we obtained the aberration equations of the inverted telephoto four configuration mirror zoom system as follows:

$$\begin{cases} A_1 = 1/20, \\ A_2 = 1/60, \\ \left(\dfrac{1}{\beta_{21}} - \beta_{21}\right) f_2' + \left(\dfrac{1}{\beta_{31}} - \beta_{31}\right) f_3' \\ \quad = \left(\dfrac{1}{\beta_{22}} - \beta_{22}\right) f_2' + \left(\dfrac{1}{\beta_{32}} - \beta_{32}\right) f_3', \\ S_{k1} = S_{11}(f_1, f_2, f_3, f_4, \beta_{21}, \beta_{31}, \beta_{41}) = 0, \qquad k = 1,2,3,4, \\ S_{k2} = S_{12}(f_1, f_2, f_3, f_4, \beta_{22}, \beta_{32}, \beta_{42}) = 0, \\ \varphi_1 < 0, \\ A_{(2-4)1} > 0, \\ A_{(2-4)2} > 0, \end{cases} \tag{7}$$

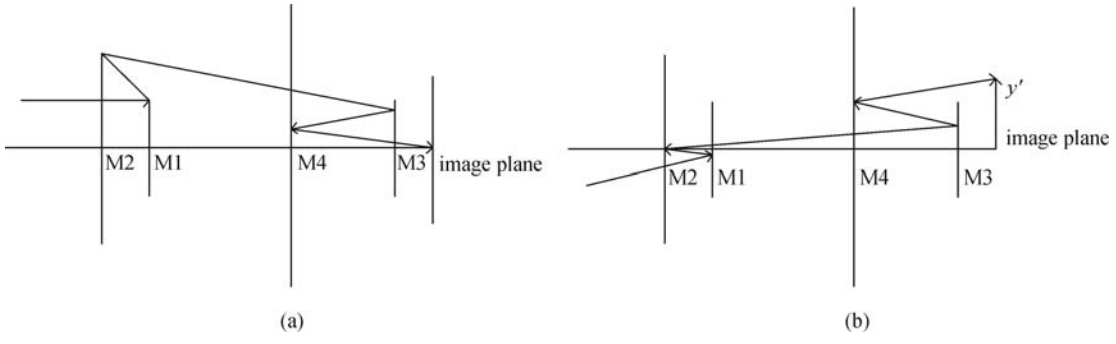

Fig. 1 (a) Marginal ray tracing of the proposed system and (b) chief ray tracing of the proposed system

where A_i (i = 1,2) is the power of the optical system of configuration i.

The initial configuration of the design was obtained by solving the expressions of the primary aberrations under specific constraints the above equation set. After comparison, we chose one most practical result, and the parameters of the proposed optical reflective zoom system are shown in Table 2.

Figure 2 is the layout of the coaxial optical zoom system. M1 is the zoom group. M2 and M3 are the fixed groups. M4 is the compensating group. The zoom group was designated as the primary mirror while the compensating group was designated as the fourth mirror.

Figure 3 is the modulation transfer function (MTF) curve of the initial configuration of the coaxial mirror zoom system. At its shorter focus position (f = 20 mm), the system acquires image quality with MTF below 0.1 at the ±3.6° field angle. And at the longer focus position (f = 60 mm), the system has the image quality with MTF above 0.5. However, it has not attained the diffraction limited image quality. Figures 4 and 5 show that the system suffers from high distortion, astigmatism and spherical aberrations. But the dominant aberration of the system to be fixed are the spherical aberration and astigmatism. After all, the system needs to be further optimized.

So, it is essential to optimize the system to reach the acceptable limit for these aberrations at different focus. Here, in order to further correct aberrations, we try to make full use of aspherical coefficients by finding the relationship between the aberration and every aspherical coefficient of the four-mirror zoom system. We obtained the relationship of the spherical aberration in the system with the conic coefficient, the 4th order coefficient, the 6th order coefficient, the 8th order coefficient and the 10th order coefficient using the aberration analysis software in ZEMAX®.

Table 2 Parameters of the initial structure of mirror zoom system

nomenclature	radius/mm	thickness/mm (f = 20 mm)	thickness/mm (f = 60 mm)
primary mirror	33.933	−9.324	−13.373
secondary mirror	44.533	67.011	67.011
tertiary mirror	41.068	−34.636	−14.891
fourth mirror	46918	37.629	17.884

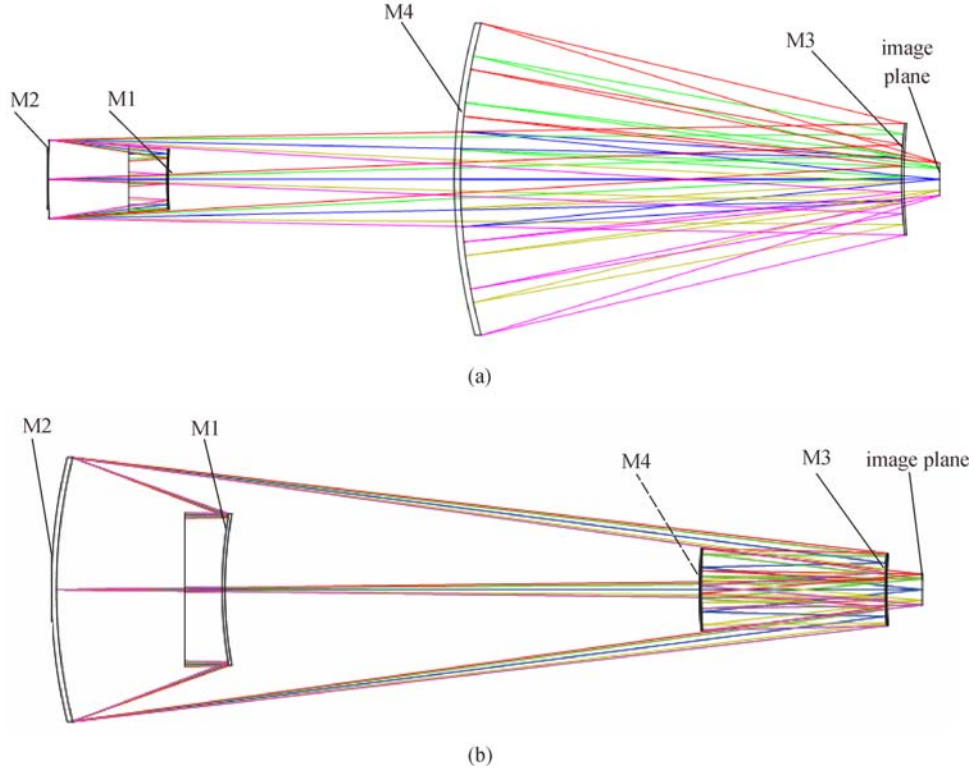

Fig. 2 Layout of coaxial mirror zoom system. (a) f = 20 mm and (b) f = 60 mm

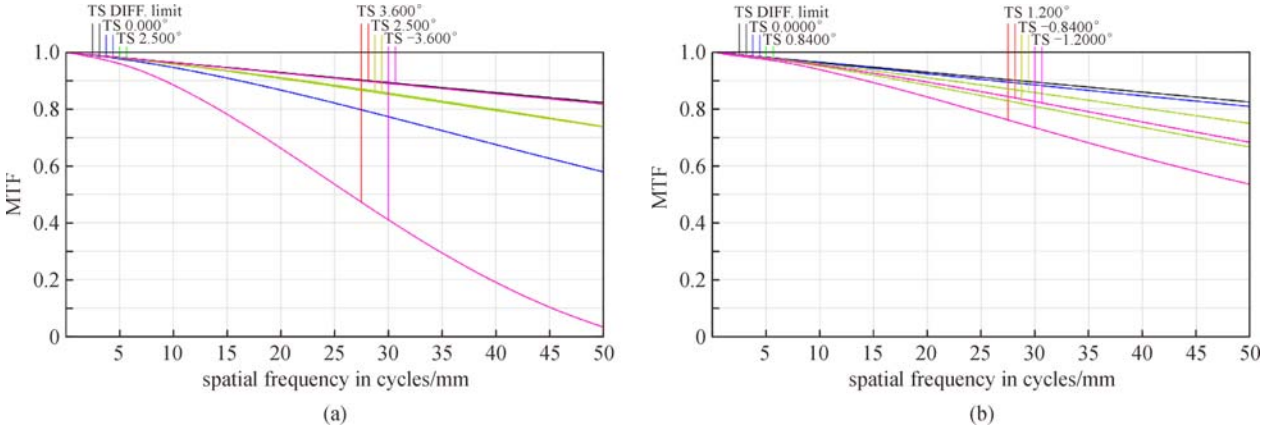

Fig. 3 Modulation transfer function (MTF) of the coaxial mirror zoom system. (a) $f = 20$ mm and (b) $f = 60$ mm

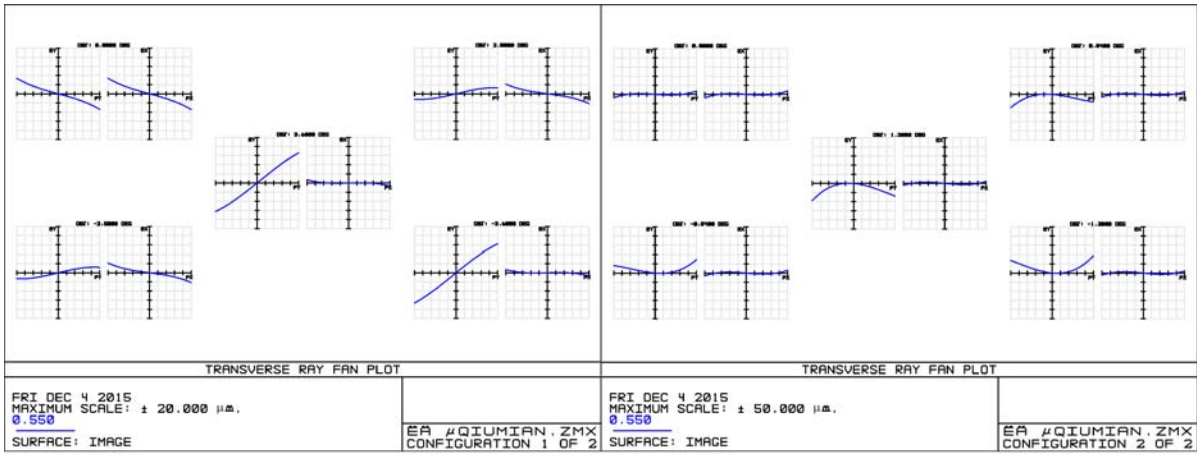

Fig. 4 Ray aberration curves of coaxial mirror zoom optical system. (a) $f = 20$ mm and (b) $f = 60$ mm

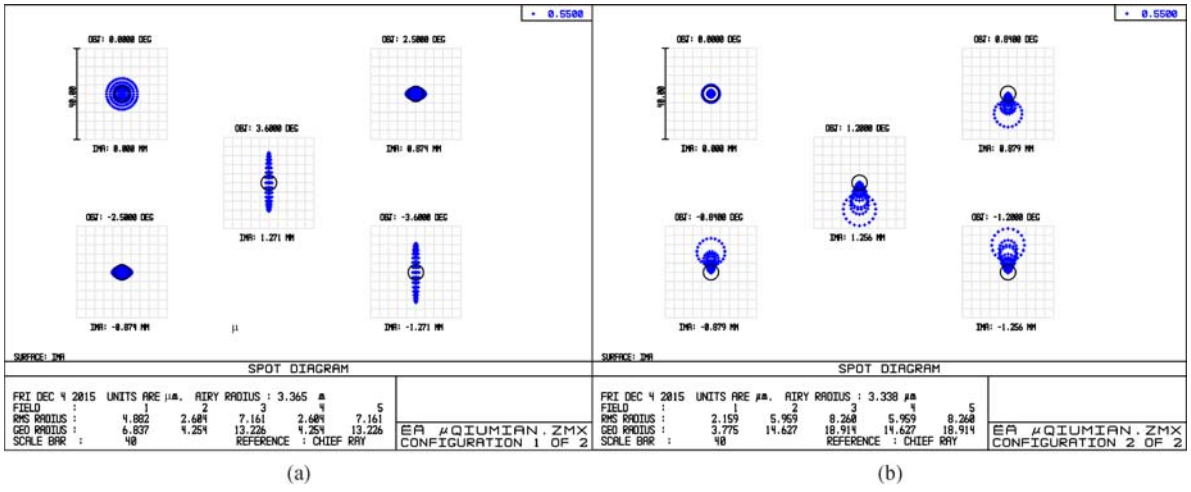

Fig. 5 Spot diagram of coaxial mirror zoom optical system. (a) $f = 20$ mm and (b) $f = 60$ mm

3 Optimization and results

An aspheric surface is commonly used to eliminate or minimize the aberrations of an optical system while increasing its FOV. Therefore we optimized our four-mirror zoom system by incorporating the aspheric coefficients with the help of ZEMAX®. Figures 6–10 show the relationship between aberration and the aspheric coefficient of each surface. The focus of the first configuration was 20 mm, while the second configuration was 60 mm.

Figure 6 illustrates how the aspheric coefficients of these four mirrors affect the spherical aberrations of these two configurations. The total spherical aberration of the first configuration was positive, while the total spherical aberration of the second configuration was negative. The conic and 4th coefficients of the tertiary and fourth mirrors could introduce a positive change to the spherical aberration of the first configuration, thus the total spherical aberration of the first configuration became larger. The conic and 4th coefficients of the primary and secondary mirrors could introduce a positive change to the spherical aberration of second configuration, the positive change of the spherical aberration of the second configuration could offset its original negative value, but the correction was a bit excessive. The 6th, 8th and 10th coefficients of the tertiary and fourth mirror imposed a little negative effect on both configurations.

Figure 7 illustrates how the aspheric coefficients of these four mirrors affect the comas of these two configurations. The coma of the first configuration was almost zero, while that of the second configuration was positive. The aspheric coefficients of the primary and secondary mirrors and 6th, 8th and 10th coefficients of the fourth mirror imposed little effect on the first configuration. The conic and 4th coefficients of the primary and secondary mirrors could introduce a negative change to the coma of second configuration, this change could offset its original positive value.

Figure 8 illustrates how the aspheric coefficients of these

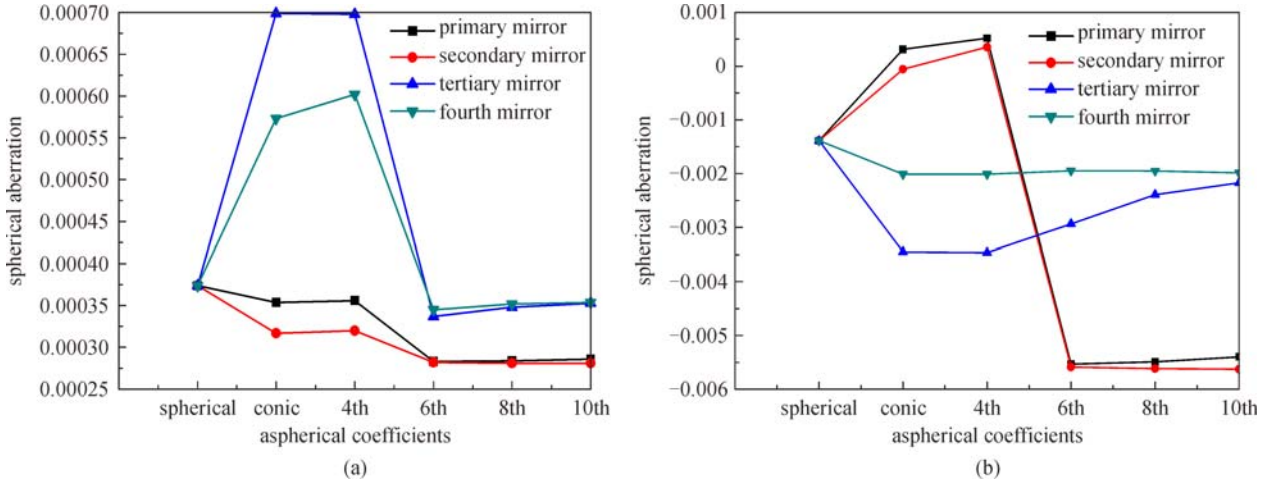

Fig. 6 Spherical aberration of (a) $f = 20$ mm and (b) $f = 60$ mm

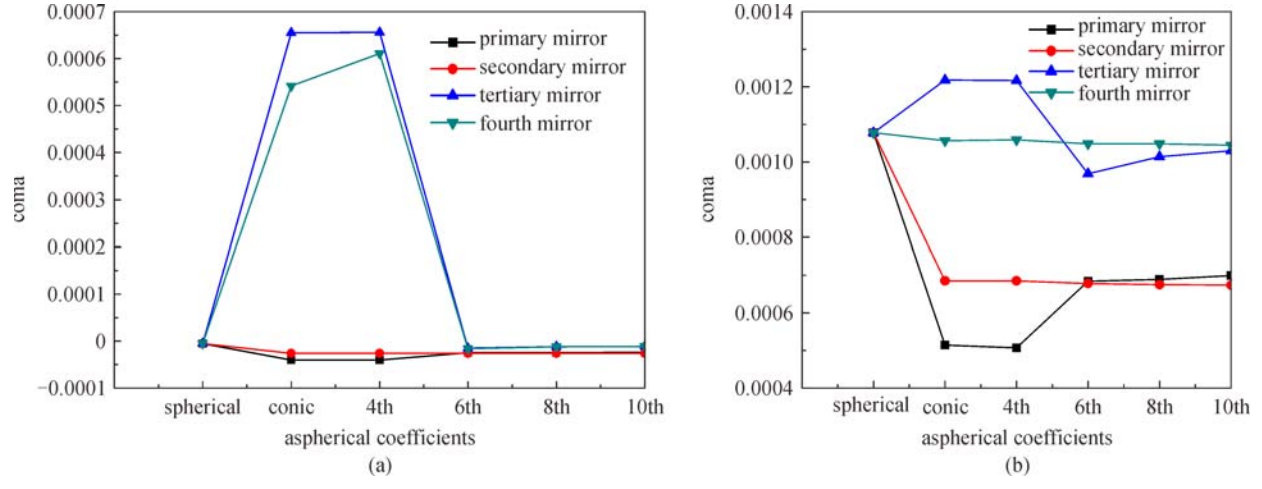

Fig. 7 Comas of (a) $f = 20$ mm and (b) $f = 60$ mm

four mirrors affect the astigmatisms of these two configurations. The astigmatism of these two configurations were negative, while the first configuration was much larger than the second one. The conic and 4th coefficients of the tertiary and fourth mirrors introduced a positive change to the astigmatism of the first configuration that could offset its original negative value.

Figure 9 illustrates how the aspheric coefficients of these four mirrors affect the field curvatures of these two configurations. The field curvatures of these two configurations were positive. The aspheric coefficients of the primary and secondary mirrors introduced a negative change to the field curvature of the both configurations that could offset its original positive value.

Figure 10 illustrates how the aspheric coefficients of these four mirrors affect the distortions of these two configurations. The distortion of the first configuration was negative, while that of the second configuration was almost zero. The influence mode was similar to the astigmatism.

To sum up, the original value of the spherical aberration was 0.00037 at the shorter focus position and –0.0014 at the longer focus. The coefficients of the primary and the secondary mirrors had similar effect on these aberrations of both configurations, but the conic and 4th coefficients of the primary mirror had better performance on balance coma, therefore we can take either conic or the 4th coefficient of the primary mirror as variables. For the third and the fourth mirror, the 6th, 8th and 10th aspheric coefficients introduced a negative change to the spherical aberration at both focus position, made the spherical aberration become smaller at the short focus position, meanwhile, compensated for the excessive correction of the primary mirror at the longer focus position. We can take either two or three of the 6th, 8th and 10th coefficients as variables.

According to the above analysis, we chose the 6th and 8th aspheric coefficients of the fourth mirror and the conic coefficient of the primary mirror as variables to optimize. The parameters and the layout of the coaxial optical zoom system after optimization are shown in Table 3 and Fig. 11 respectively. The ray aberration, the spot diagram and the MTF of the coaxial mirror zoom system after optimization

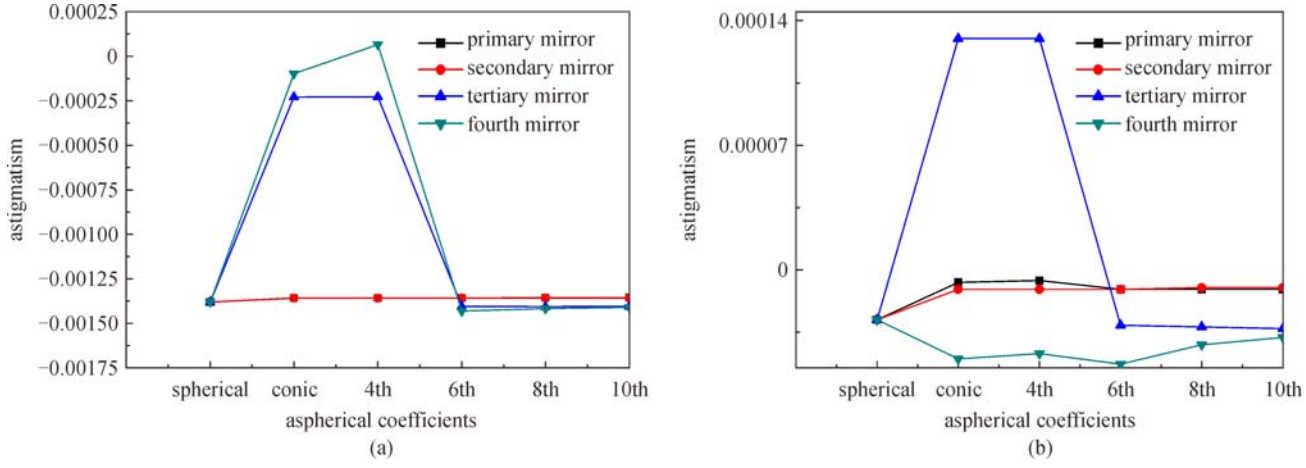

Fig. 8 Astigmatisms of (a) f = 20 mm and (b) f = 60 mm

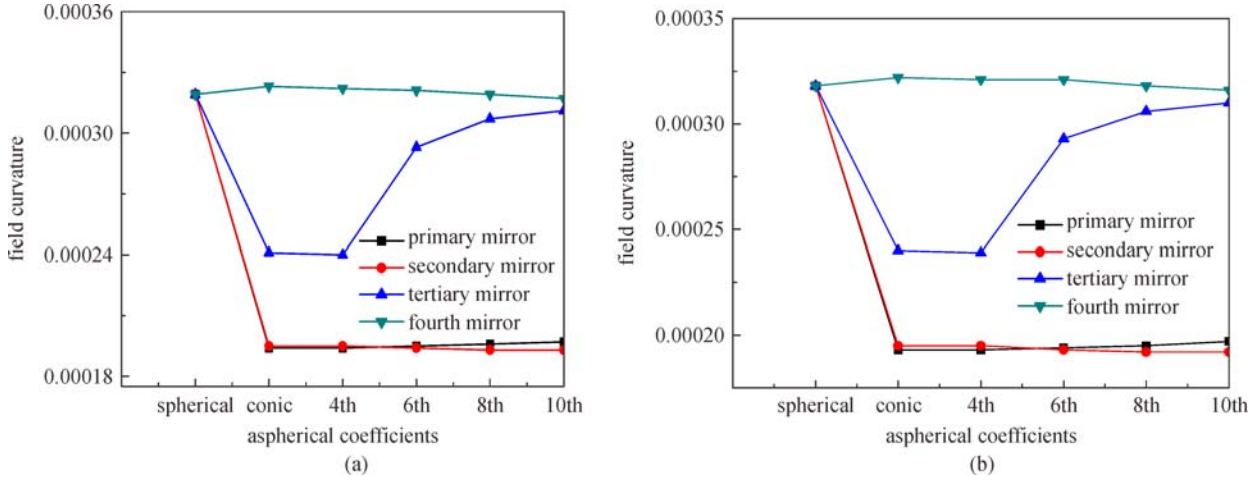

Fig. 9 Field curvatures of (a) f = 20 mm and (b) f = 60 mm

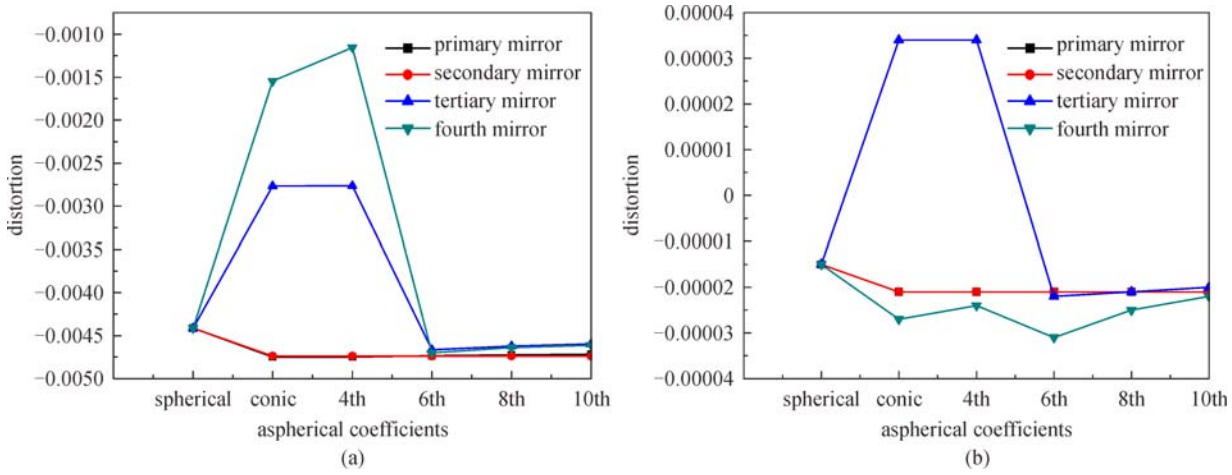

Fig. 10 Distortions of (a) $f = 20$ mm and (b) $f = 60$ mm

Table 3 Parameters of the final optical zoom system

nomenclature	radius/mm	thickness/mm ($f = 20$ mm)	thickness/mm ($f = 60$ mm)	aspherical coefficients				
				conic	4th	6th	8th	10th
primary mirror	42.028	−7.332	−12.393	−0.3347	0	0	0	0
secondary mirror	45.930	59.910	58.913	0	0	0	0	0
tertiary mirror	32.390	−28.991	−14.048	0	0	0	0	0
fourth mirror	39.263	31.9422	19.048	0	0	1.7403E−009	−6.199E−012	0

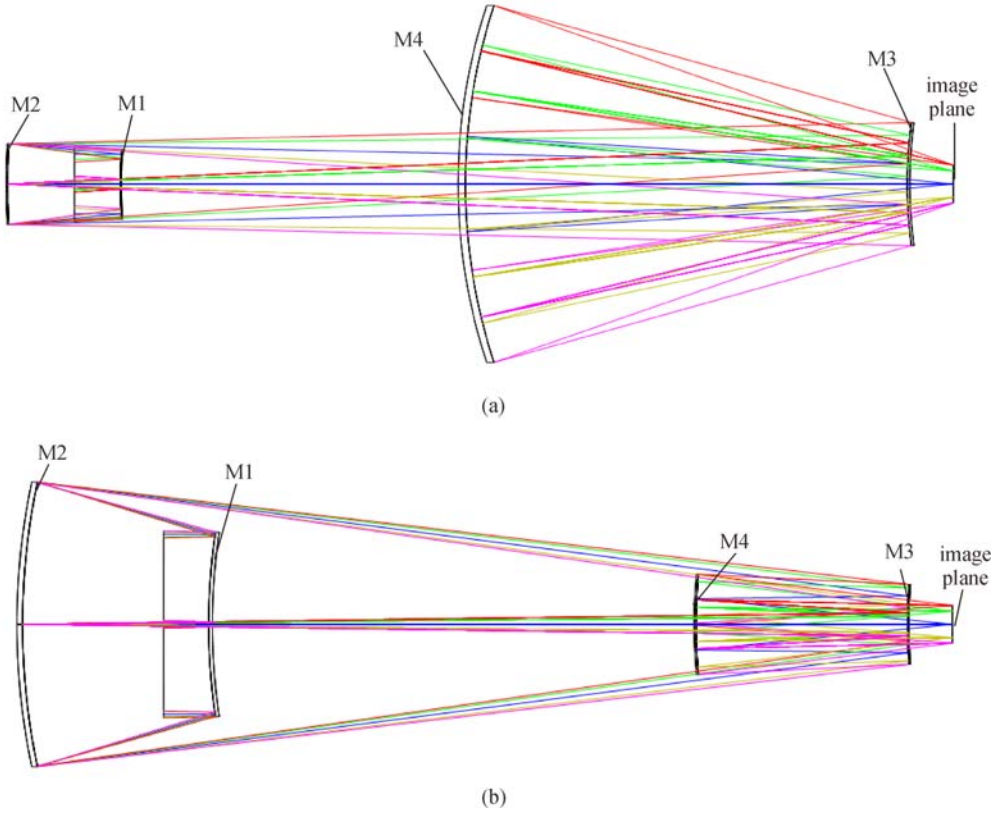

Fig. 11 Layout of the coaxial optical zoom system after optimization. (a) $f = 20$ mm and (b) $f = 60$ mm

are shown in Figs. 12–14 respectively.

From the ray aberration curves, the aberration scale after optimization was much smaller than that of the initial structure, the spot diagrams show that the root mean square (RMS) radius were less than the airy radius after optimization, and Fig. 14 shows the system after

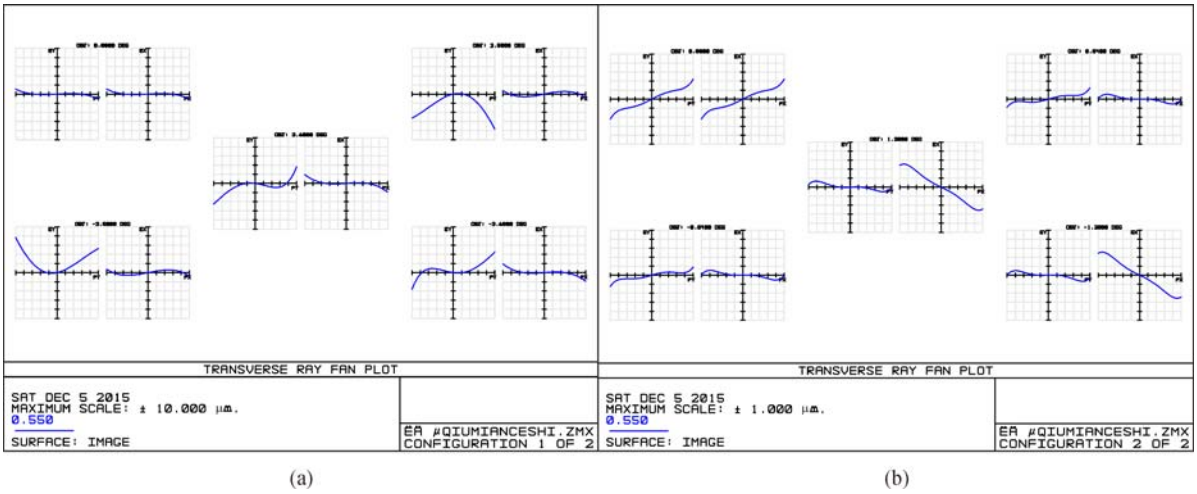

(a) (b)

Fig. 12 Ray aberration curves of coaxial mirror zoom optical system after optimization. (a) f = 20 mm and (b) f = 60 mm

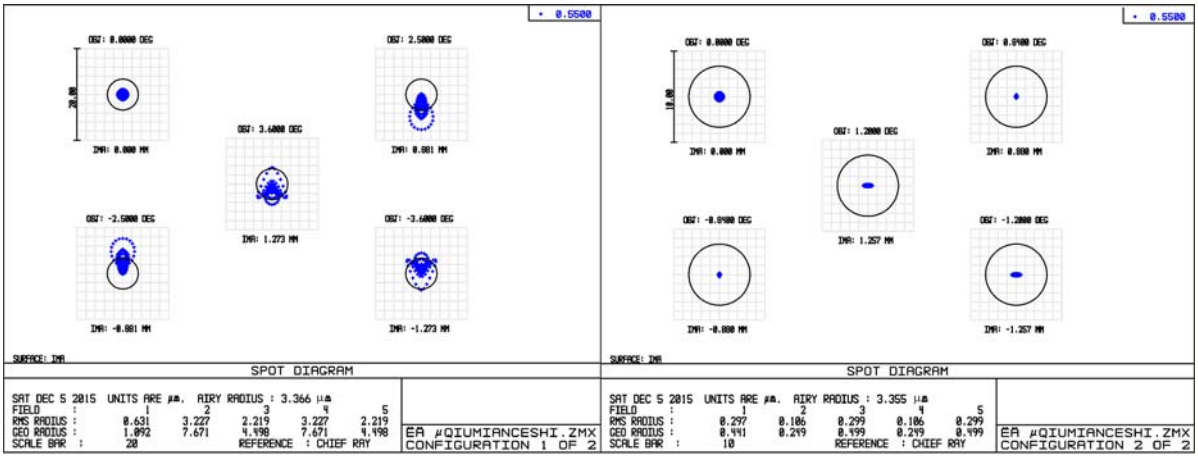

(a) (b)

Fig. 13 Spot diagram of the optical zoom system after optimization. (a) f = 20 mm and (b) f = 60 mm

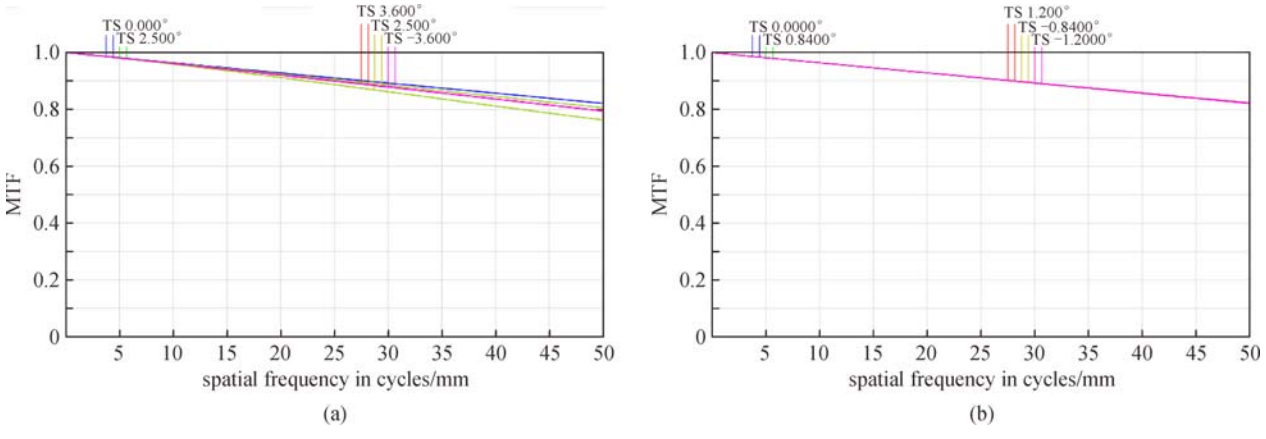

(a) (b)

Fig. 14 Diffraction limited MTF of the optical zoom system after optimization. (a) f = 20 mm and (b) f = 60 mm

optimization had almost attained the diffraction limited image quality.

4 Conclusion

In this paper, we developed the initial configuration of the four mirror inverted telephoto zoom system by solving aberration equations with specific constraints, and analyzed the relations between aspheric coefficients and aberrations. With the help of these relations, we can use the specific aspherical coefficient to balance the specific aberration not only in this one system, but also in other systems like this kind. Finally, we obtained the diffraction limited image quality by using two aspheric surfaces in our design. Such reflective optical zoom systems can accomplish the requirements of broad spectrum and wide FOV.

Acknowledgements This research work was financially supported by the National Natural Science Foundation of China (Grant No. 61178041) and Pre-Research Foundation (No. 201511340836).

References

1. Seidl K, Knobbe J, Grüger H. Design of an all-reflective unobscured optical-power zoom objective. Applied Optics, 2009, 48(21): 4097–4107
2. Seidl K, Knobbe J, Schneider D, Lakner H. Distortion correction of all-reflective unobscured optical-power zoom objective. Applied Optics, 2010, 49(14): 2712–2719
3. Hu S L, Zhao X, Dong W H, Xie Y J. Active optical system for any field angle zoom. Optical Engineering (Redondo Beach, Calif.), 2011, 50(11): 1–5
4. Dong W H, Xie Y J, Li E L. Design of coaxial catadioptric zoom system using deformable mirrors. Applied Optics, 2010, 31(6): 893–897
5. Lin Y H, Liu Y L, Su G D J. Optical zoom module based on two deformable mirrors for mobile device applications. Applied Optics, 2012, 51(11): 1804–1810
6. Du X, Chang J, Zhang Y, Wang X, Zhang B, Gao L, Xiao L. Design of a dynamic dual-foveated imaging system. Optics Express, 2015, 23(20): 26032–26040
7. Wang D, Wang Q, Shen C, Zhou X, Liu C. Color holographic zoom system based on a liquid lens. Chinese Optics Letters, 2015, 13(7): 072301–072305
8. Mikš A, Novák J, Novák P. Method of zoom lens design. Applied Optics, 2008, 47(32): 6088–6098
9. Zhang T C, Wang Y T, Chang J, Talha M M. Design of reflective zoom system with three mirrors. Acta Optica Sinica, 2010, 30(10): 3034–3038
10. Zhang T C, Liu L P, Chang J, Wang Y T. Design of infrared zoom systems with 4 reflective mirrors. Journal of Infrared and Millimeter Waves, 2010, 29(3): 196–200
11. Yan P, Fan X. New design of an off-axis reflective zoom optical system. Infrared & Laser Engineering, 2012, 41(6): 1581–1586

Jun Chang is a Professor and PhD Supervisor of School of Optoelectronic at Beijing Institute of Technology. He received his PhD degree in optics from Changchun University of Science and Technology in 2002. He has 13 years experience in reflective zoom optical system, reflective zoom optical system based on active optics, high precision detection of the offset state of micro system assembly, design of the universal compensator for testing aspheric surfaces and short baseline distance and long detecting distance measurement with binocular vision based on Opencv. He is the author of more than 60 journal papers. His current interests include optical design and measurement, and electro-optical countermeasures.

Guijuan Xie obtained her bachelor's degree in optical information science and technology from Anhui University in 2013, and she has been a MS candidate at School of Optoelectronic, Beijing Institute of Technology since 2013. Her current research is optical design.

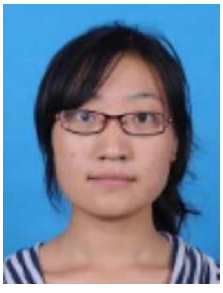

Lifei Zhang obtained her bachelor's degree in optical information science and technology from Anhui University in 2010, and she has been a MS candidate at School of Optoelectronic, Beijing Institute of Technology since 2010. She received her MS degree in 2013. Her current research is optical design.

Yao Xu obtained his bachelor's degree from Beijing University of Technology in 2012, and he has been a MS candidate at School of Optoelectronic, Beijing Institute of Technology since 2012. He received his MS degree in 2015. His current research is optical design.

Jide Zhou obtained his bachelor's degree in optical information science and technology from Huadong East China Jiaotong University in 2013, and he has been a MS candidate at School of Optoelectronic, Beijing Institute of Technology since 2013. He received his MS degree in 2016. His current research is optical design.

Shengyi Yang is a Professor and PhD Supervisor of School of Physics at Beijing Institute of Technology. He received his PhD degree from Beijing Jiaotong University in 2001. He has 14 years experience in photodetectors, solar cells and light-emitting diodes. His current interests include optoelectronic materials and devices, nano photonics materials in photodetectors, light emitting transistor, solar cells, and other optoelectronic devices.